



Review

# Effects of Steel Fiber Percentage and Aspect Ratios on Fresh and Harden Properties of Ultra-High Performance Fiber Reinforced Concrete

Rajib Kumar Biswas <sup>1,\*</sup>, Farabi Bin Ahmed <sup>2,†</sup>, Md. Ehsanul Haque <sup>2</sup>, Afra Anam Provasha <sup>2</sup>, Zahid Hasan <sup>2</sup>, Faria Hayat <sup>2</sup> and Debasish Sen <sup>2</sup>

<sup>1</sup> Department of Civil and Environmental Engineering, Tokyo Institute of Technology, 2-12-1-M1-21, Ookayama, Meguro-ku 152-8552, Japan

<sup>2</sup> Department of Civil Engineering, Ahsanullah University of Science and Technology, Tejgaon, Dhaka Industrial Area, Dhaka 1208, Bangladesh; 160103056@aust.edu (F.B.A.); 160103064@aust.edu (M.E.H.); 160103111@aust.edu (A.A.P.); 160103062@aust.edu (Z.H.); 170103164@aust.edu (F.H.); debasish.ce@aust.edu (D.S.)

\* Correspondence: rajib.k.aa@m.titech.ac.jp

† These authors contributed equally to this work.

**Abstract:** Steel fibers and their aspect ratios are important parameters that have significant influence on the mechanical properties of ultrahigh-performance fiber-reinforced concrete (UHPFRC). Steel fiber dosage also significantly contributes to the initial manufacturing cost of UHPFRC. This study presents a comprehensive literature review of the effects of steel fiber percentages and aspect ratios on the setting time, workability, and mechanical properties of UHPFRC. It was evident that (1) an increase in steel fiber dosage and aspect ratio negatively impacted workability, owing to the interlocking between fibers; (2) compressive strength was positively influenced by the steel fiber dosage and aspect ratio; and (3) a faster loading rate significantly improved the mechanical properties. There were also some shortcomings in the measurement method for setting time. Lastly, this research highlights current issues for future research. The findings of the study are useful for practicing engineers to understand the distinctive characteristics of UHPFRC.

**Keywords:** fiber percentage; aspect ratio; setting time; workability; loading rate



**Citation:** Biswas, R.K.; Bin Ahmed, F.; Haque, M.E.; Provasha, A.A.; Hasan, Z.; Hayat, F.; Sen, D. Effects of Steel Fiber Percentage and Aspect Ratios on Fresh and Harden Properties of Ultra-High Performance Fiber Reinforced Concrete. *Appl. Mech.* **2021**, *2*, 501–515. <https://doi.org/10.3390/applmech2030028>

Received: 10 June 2021

Accepted: 19 July 2021

Published: 21 July 2021

**Publisher's Note:** MDPI stays neutral with regard to jurisdictional claims in published maps and institutional affiliations.



**Copyright:** © 2021 by the authors. Licensee MDPI, Basel, Switzerland. This article is an open access article distributed under the terms and conditions of the Creative Commons Attribution (CC BY) license (<https://creativecommons.org/licenses/by/4.0/>).

## 1. Introduction

Concrete is a very popular construction material (its annual consumption is about 25 billion tons) because of its low cost, availability, long durability, easily given shape and size, and ability to be sustained in extreme weather conditions [1]. On the other hand, concrete has a number of problems that cause considerable concern in the construction industry. Concrete is a brittle material with low tensile strength (approximately 1/10 of its compressive strength) [2]. In addition to its low tensile strength, concrete fracture toughness is at least 100 times less than that of steel. Moreover, concrete elements have a low capacity for resisting cracks under dynamic loads [3]. Consequently, these factors allow concrete structures to easily grow cracks during service life, create access for deleterious agents, and ultimately lead to steel bar corrosion [3–8]. Conventional concrete with low strength and a brittle nature creates concerning issues such as the durability and large section sizes of RC and prestressed structures [9–12]. To overcome the limitations of conventional concrete, a new scope of research was created to develop a cementitious composite having ultrahigh compressive strength, low porosity, and high ductility. Substantial research has been carried out to develop this technology, and it is known as ultrahigh-performance fiber-reinforced concrete (UHPFRC).

The development of UHPFRC began as ultrahigh-strength cement pastes. In 1972, Yudenfreund et al. [13] and Roy et al. [14] first produced ultrahigh-strength cement pastes

with low porosity. Yudenfreund et al. [13] achieved about 240 MPa of compressive strength, using 0.2 water to binder ratios at 25 °C. Roy et al. [14] applied (1) hot pressure (25 to 50 ksi pressure at nearly 100 °C) and (2) high pressure (100 ksi pressure) to the concrete mix, and it resulted in 59.3 and 46.1 ksi compressive strength, respectively. The development of UHPFRC reached advanced stages after the 1980s. Alford and Birchall [15] and Bache [16] used densified small particles (DSP) and macro defect-free (MDF) paste concepts to develop UHPFRC. In 1994, De Larrard and Sedran [17] applied a 0.14 water-to-binder proportion and packing-density concept to develop flowable cement–mortar composite pastes with 236 MPa of compressive strength. Lastly, Richard and Cheyrezy [18] introduced ultrahigh-strength ductile concrete designated as reactive-powder concrete (RPC), which was the forerunner of UHPFRC. Richard and Cheyrezy [18] demonstrated that ultrahigh strength and toughness could be achieved by optimizing granular materials, using the packing-density method, where the concrete mix was subjected to heat from 20 to 400 °C and pressure at 50 MPa. Maximal compressive strength of 810 MPa was obtained by incorporating 3% steel fibers. Following the successful production of UHPFRC under laboratory conditions, various researchers attempted to produce it without any distinguishing characteristics. Various researchers attempted to produce UHPFRC with special treatments such as heat curing, high pressure, and extensive vibration [19–21]. UHPFRC was recently successfully implemented in large-scale RC structures and for retrofitting structural elements such as beams, columns, and bridge piers [22–26].

Other than having high strength, UHPFRC has a number of advantages, i.e., the dense matrix improves the durability of concrete [18,27]; for the same external load, it offers one-third or one-half the section size of conventional concrete [28], and it is more ecofriendly compared to traditional concrete, owing to fewer emissions of greenhouse gases [29–34]. Even though UHPFRC has numerous advantages, its applications are very limited, owing to higher manufacturing costs than those of conventional concrete. Therefore, the application of UHPFRC with low production costs is a major challenge. There are a couple of methods that may reduce the manufacturing costs of UHPFRC: (1) decreasing or optimizing the percentage of steel fibers without deteriorating the mechanical properties [35,36] and (2) avoiding a heat or high-pressure compaction approach [19,37].

Several researchers have attempted to improve the mechanical properties of UHPFRC by increasing the aspect ratio rather than the fiber dosage [38–40]. Therefore, the primary research goals of this study are summarizing the available experimental results regarding the effects of the steel fiber percentage and aspect ratio on the fresh and hardened properties of UHPFRC, i.e., setting time, slump or workability, compressive strength, tensile strength, crack control, and ductility as well as assisting engineers in understanding the distinctive characteristics of UHPFRC and optimizing the fiber dosage and aspect ratio of steel fibers. This research also highlights current challenges and major needs for future research.

## 2. Characteristics of Fresh UHPFRC

### 2.1. Effect of Steel Fiber Percentages and Aspect Ratio on Setting Times

The setting time of concrete is crucial for construction work, as it is associated with the removal of formwork, the construction schedule, etc. The outer surface of an UHPFRC specimen (exposed to weather) has a much faster evaporation rate of water than that of the inner part. This rapid evaporation of surface moisture misrepresents measurements of UHPFRC setting time, following the ASTM C403 [41] penetration resistance testing method. Yoo et al. [42] applied various methods and materials and suggested that using paraffin oil might resist water evaporation during the penetration resistance test. Consequently, accurate initial and final setting times for UHPFRC were found to be 10.8 and 12.3 h, respectively, as shown in Figure 1. Zhang et al. [43] demonstrated that for an identical mix design, initial setting times were delayed from 670 to 1165 min, and final setting times were delayed from 1010 to 1915 min when the volumetric steel fiber ratio increased from 1% to 3%, as shown in Table 1. Results indicated that the increased steel fiber amount had

a negative effect on setting time. Very limited research has been performed to understand the effect of the fiber percentage on the setting time.

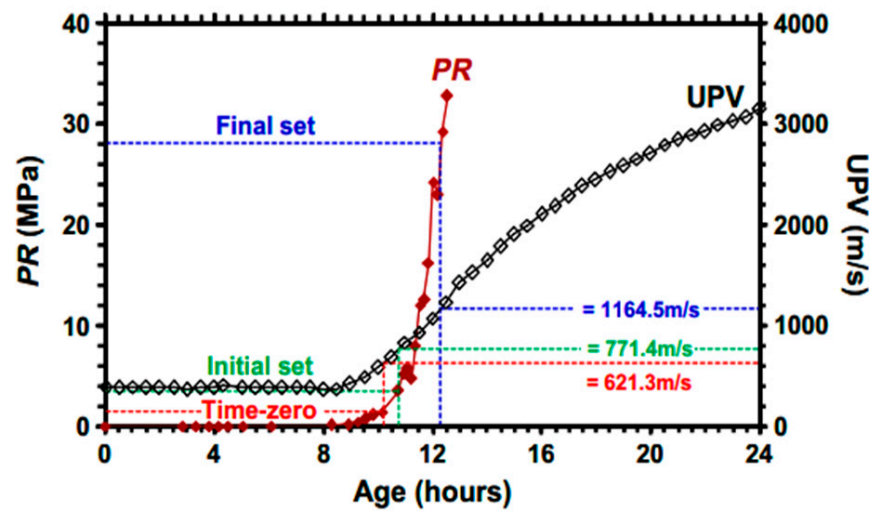


Figure 1. Comparison of penetration resistance of UHPFRC [42].

Table 1. Effect of fiber percentage on setting times [43].

| Sample Name | Temperature (°C) | Binder Composition (%) |    |    |    | Binder and Sand Ratio | Sand and Aggregate Ratio | Fiber Percentage | Setting Times (Min) |       |
|-------------|------------------|------------------------|----|----|----|-----------------------|--------------------------|------------------|---------------------|-------|
|             |                  | C                      | Fa | Sf | SI |                       |                          |                  | Initial             | Final |
| SFRC6       | 90               | 50                     | 10 | 10 | 30 | 1:1                   | 1:1                      | 1                | 670                 | 1010  |
| SFRC7       | 90               | 50                     | 10 | 10 | 30 | 1:1                   | 1:1                      | 2                | 1030                | 1430  |
| SFRC8       | 90               | 50                     | 10 | 10 | 30 | 1:1                   | 1:1                      | 3                | 1165                | 1915  |

### 2.2. Effects of Steel Fiber Percentages and Aspect Ratios on Slump or Workability

Owing to its low w/b ratio, UHPFRC demonstrates low flowability, which causes difficulty during casting. In addition, an increase in steel fibers affects the workability of UHPFRC. Svec and Pade [44] observed that the flow of UHPFRC significantly decreased with the increase in steel fiber percentage, as depicted in Figure 2. An interlocking issue was encountered when the steel fiber percentage reached 8%. Similarly, several other researchers also reported that an increased fiber percentage negatively impacted slump flow [45–47]. Another study by Yu et al. [48] revealed that relative slump flow linearly decreased with an increase in steel fiber percentage (0.5% to 2.5%; Figure 3). The main reason for the reduced slump is summarized as follows:

- An increased steel fiber amount creates interlocking among steel fibers and ultimately leads to reduced workability [48];
- If the length of fiber is more than the aggregate size, the surface area of the fiber becomes larger and creates a cohesive force between fibers [48].

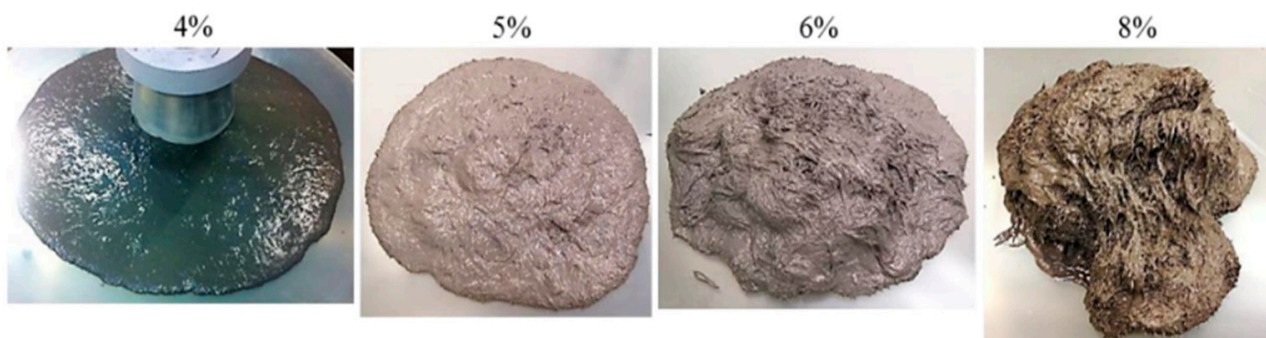


Figure 2. Effect of steel fiber percentage on UHPFRC workability [44].

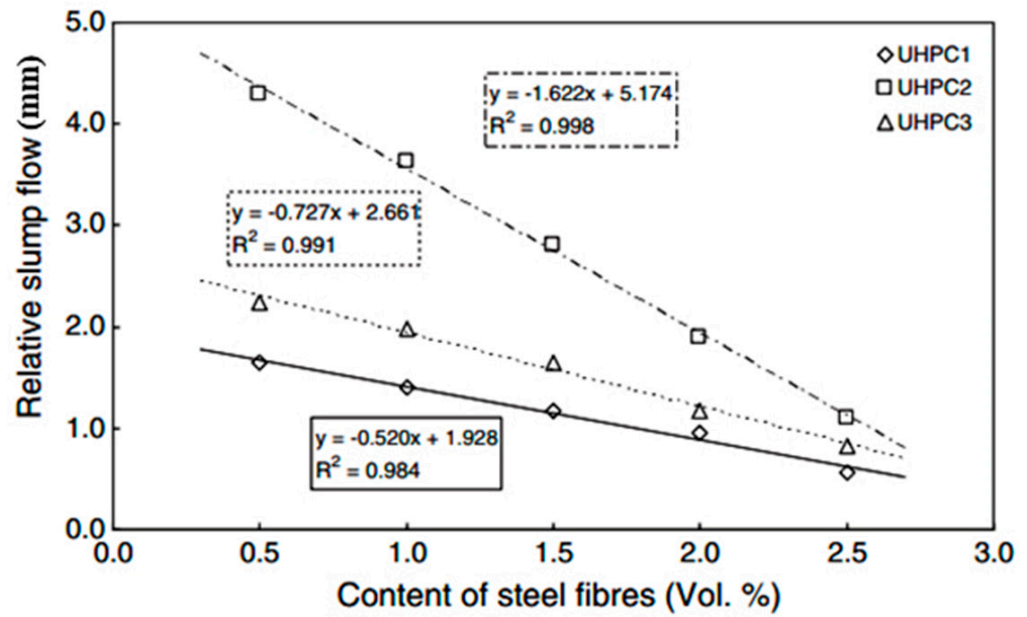


Figure 3. Relation between slump flow and fiber content [48].

Hoang and Fehling [49] investigated the effects of fiber percentage (0%, 1.5%, and 3%) and aspect ratio (13/0.175, 20/0.25, and 9/0.15) on  $t_{500}$  (the time required for UHPFRC to spread 500 mm dia) and slump flow (Figures 4 and 5). Fiber percentage and aspect ratio (L/D) increments reduced slump flow and increased  $t_{500}$ . Several other researchers also reported that an increased fiber aspect ratio negatively impacted slump flow [47,50]. Wille et al. [20] reported that UHPFRC mixtures containing steel fibers with a low aspect ratio (6 mm long and 0.15 mm diameter) were more workable, and steel fibers could be used up to 10%. Rossi [51] found that 12 mm long and 0.15 mm diameter fibers that used up to 3% of the total concrete volume could be used without affecting mixture workability. Alternatively, Wu et al. [52] and Yu et al. [53] reported that considering an identical amount of steel fiber, a higher aspect ratio (both researcher teams used 13/0.2) demonstrated increased flowability compared to that of steel fibers with low aspect ratios (6/0.2 and 6/0.16).

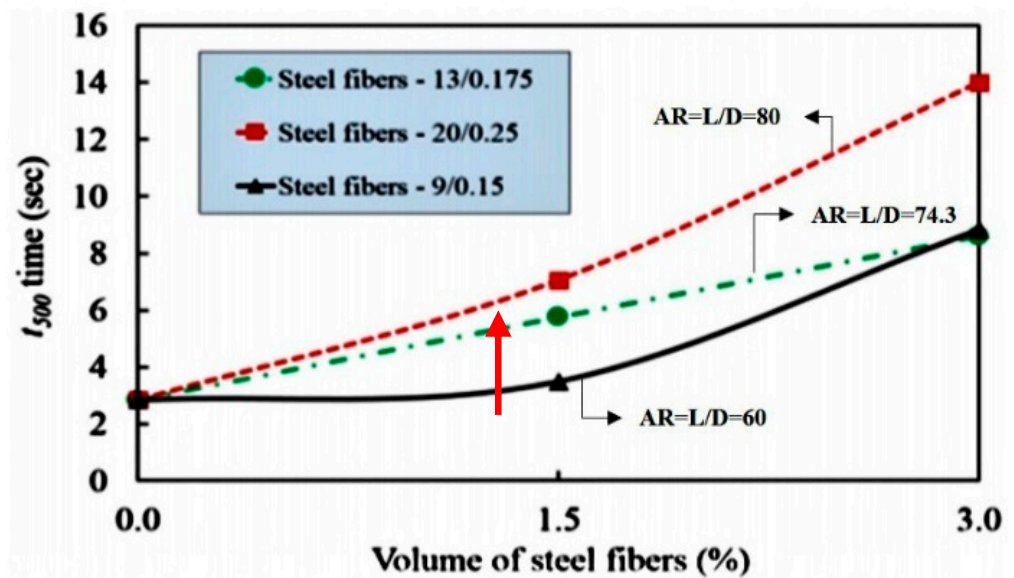


Figure 4.  $t_{500}$  for different fiber percentages and aspect ratios [49].

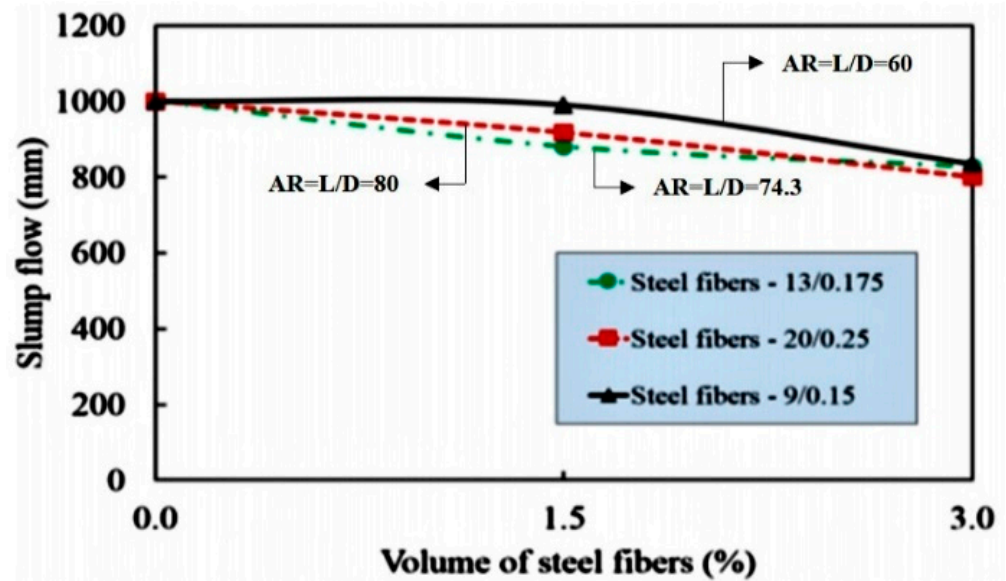


Figure 5. UHPFRC slump flow for different fiber percentages and aspect ratios [49].

### 3. Mechanical Characteristics of UHPFRC

#### 3.1. Effects of Steel Fiber Percentages and Aspect Ratios on Compressive Behavior

Experimental studies regarding the effects of steel fibers on the compressive strength of UHPFRC have not been in agreement. Some studies reported that the compressive strength of UHPFRC was not influenced or was negatively influenced by an increase in fiber percentage [45,54,55]. The researchers highlighted that due to the lack of a homogeneous distribution of steel fiber, a large amount of steel fibers encountered fiber bundling that eventually led to weak spots in the mixture. This decreased the efficiency of the concrete matrix and ultimately resulted in reduced compressive strength [45,55,56]. For instance, Hoang and Fehling [49] tested UHPFRC samples having various steel fiber percentages and aspect ratios and expressed that the addition of fiber percentages to UHPFRC negatively impacted compressive strength, as depicted in Figure 6. This research underlined that an increased fiber percentage might lead to a reduction in the compressive strength of UHPFRC of up to 7% in contrast to the no-fiber case, owing to improper fiber distribution in the concrete matrix.

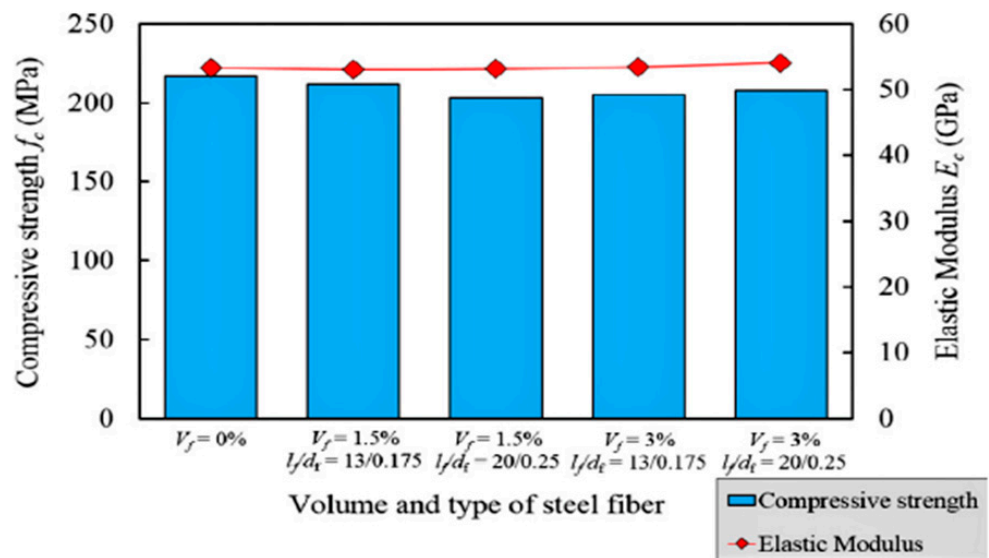


Figure 6. Negative effects of fiber dosage on the compressive strength of UHPFRC [49].

On the other hand, several researchers reported that the compressive strength of UHPFRC substantially increased (see Figure 7) with an increase in steel fibers [47,48,57–59]. Steel fibers delay concrete crack propagation and formation and ultimately result in higher strength properties [60,61]. Kazemi and Lubell [62] found a positive effect from the incorporation of steel fibers when following the ASTM C109/C109M-07 [63] and ASTM C39/C39M-10 [64] standards. In addition to compressive stress improvement, researchers also reported that an increased fiber percentage improved peak strain, which indicated ductile behavior and altered the failure pattern [65].

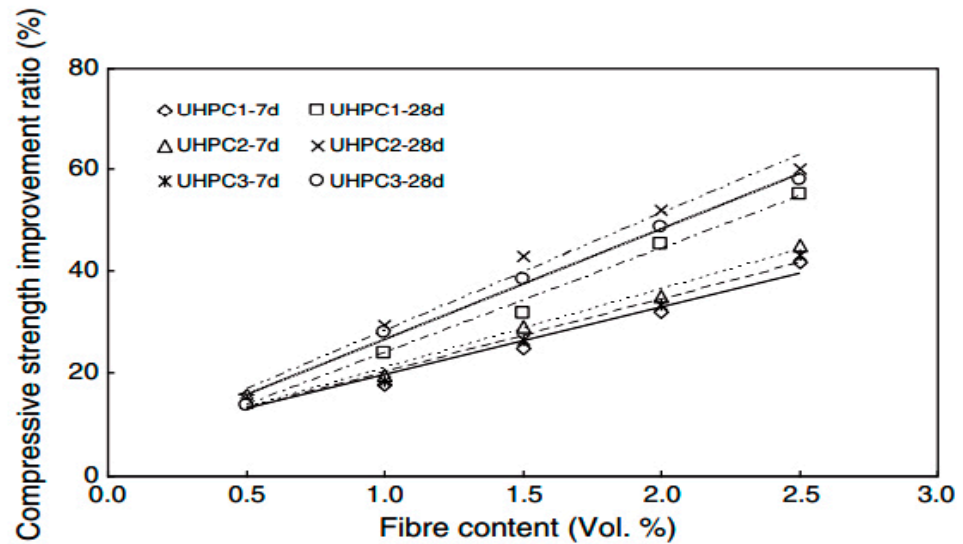


Figure 7. Relation between the steel fiber content and compressive strength of UHPFRC [49].

Previous studies have revealed that the aspect ratio of steel fibers notably influenced the compressive strength of UHPFRC. With a constant steel fiber amount, a higher steel fiber aspect ratio corresponded to better compressive strength [47,50,52,53]. Steel fibers with a high aspect ratio resisted large cracks and thus improved compressive strength; in contrast, steel fibers with a low aspect ratio could only control the opening and propagation of microcracks. Su et al. [66] used two types of steel fibers for different aspect ratios (MF06 = 50, MF15 = 125, TF03 = 100, TF05 = 60). The experiment showed that with a constant steel percentage (2.5%), steel fibers with a lower aspect ratio had lower compressive strength compared to that of steel fibers with a higher aspect ratio. The behavior was the same for both twisted and straight steel fibers, as illustrated in Figure 8a,b.

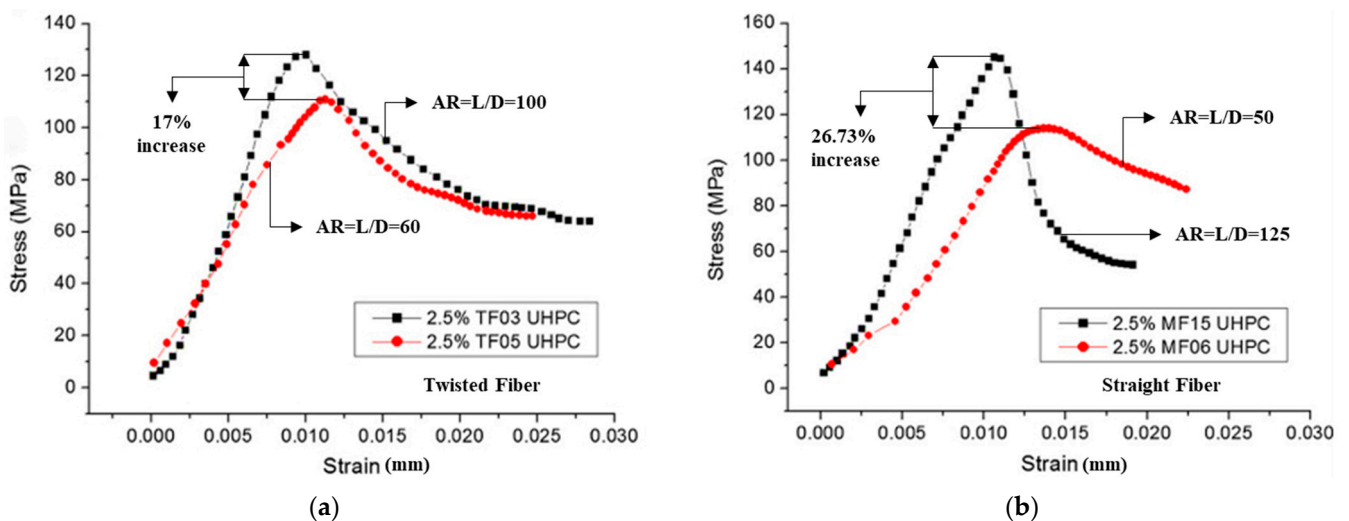
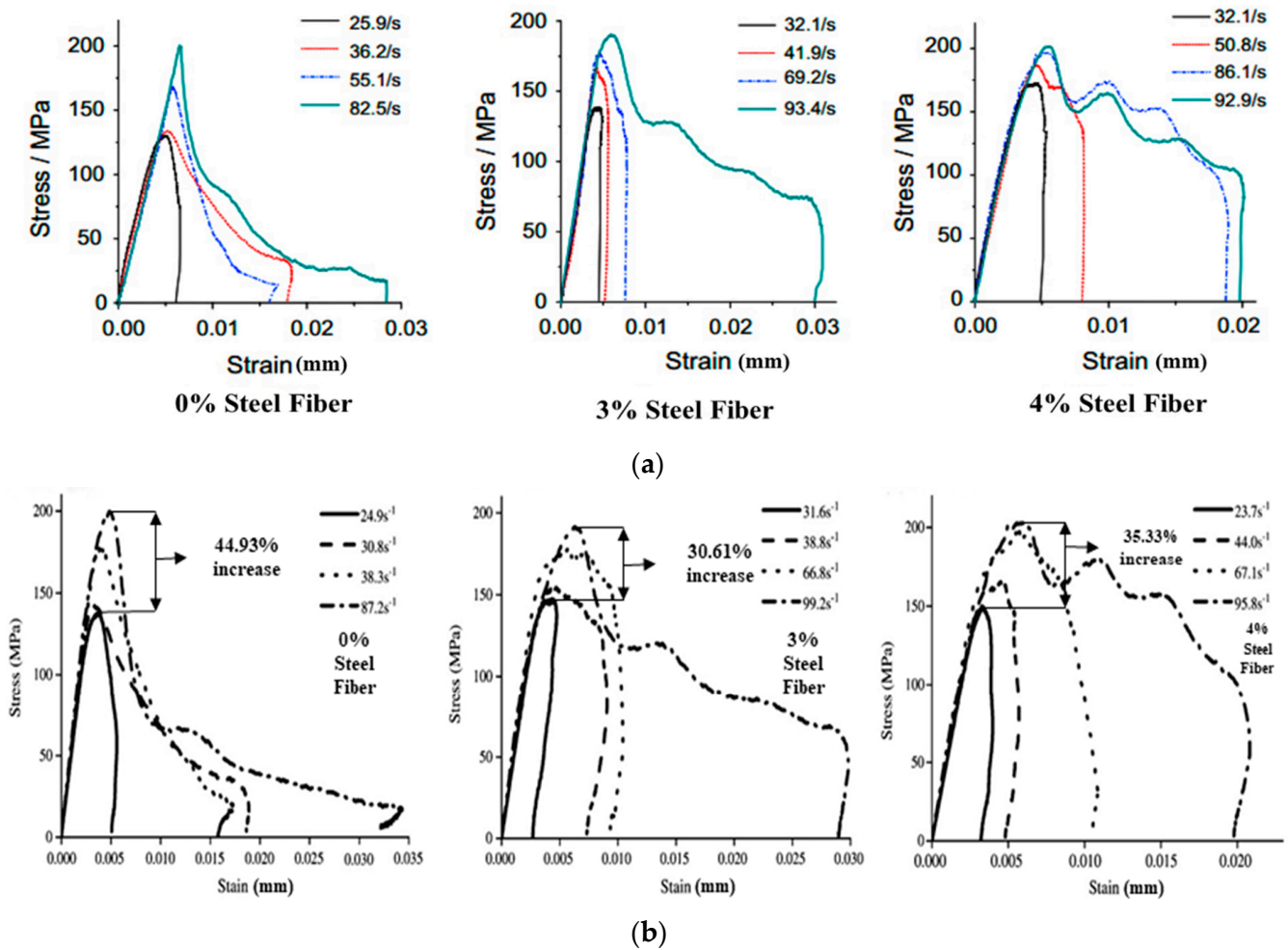


Figure 8. Effect of aspect ratio on compressive strength of UHPFRC: (a) twisted- and (b) straight-type fibers [66].

Several researchers have examined the effect of steel fiber percentage on the dynamic compressive behavior of UHPFRC under different strain rates [57,67]. Rong et al. [57] and Lai and Sun [67] examined the dynamic compressive behavior of a steel fiber dosage of up to 4%. Test results revealed that (1) the stress–strain relationship of UHPFRC was linear until ultimate strength was reached, as shown in Figure 9a; (2) an increased steel fiber amount improved the peak strain, maximal compressive strength, and elastic modulus of the concrete specimens, as shown in Figure 9b. Those experiments also found that a higher strain rate was associated with improved compressive strength.



**Figure 9.** Stress-strain response at different strain rates: (a) fiber percentage (0%, 3%, 4%); (b) fiber percentage (0%, 3%, 4%) [58,68].

Different strain rates also influence the compressive strength of UHPFRC with different steel fiber aspect ratios. For instance, Su et al. [66] examined the impact of the aspect ratio of steel fibers for different strain rates (60 and 80 s<sup>-1</sup>) with a constant steel fiber percentage. Samples with a higher aspect ratio exhibited improved compressive strength; in contrast, samples having steel fibers with a lower aspect ratio exhibited notably reduced compressive strength, as shown in Figure 10.

### 3.2. Effects of Steel Fiber Percentages and Aspect Ratios on Flexural Strength

Several researchers also examined the effect of fiber percentage on the flexural strength of UHPFRC and found that it significantly improved flexural UHPFRC strength [47,58,59,68]. An increased fiber dosage provides a larger bonding area between the concrete matrix and fibers and results in the effective control of crack propagation [47,69]. Yu et al. [48] established a relation between flexural strength and fiber percentage, as shown in Figure 11. The relation between flexural strength and steel fiber percentage was parabolic. Figure 11

shows that there was sharp flexural strength improvement for specimens with more than 1.5% steel fiber. Kazemi and Lubell [62] tested the flexural strength of UHPFRC according to ASTM C1609/C1609M-10 [70] and ASTM C1018-97 [71] with 2% to 5% of steel fiber. Flexural strength was improved by up to 107% when fiber percentage increased from 2% to 5%. However, Yoo et al. [45,69], Park [68], and Wu [72] observed no significant change in the first cracking load for specimens with increased fiber percentage. This happened because the first cracking stress was determined on the basis of the matrix strength of UHPFRC. At that stage, steel fibers had no influence because there was no fiber bridging effect, as Figures 12a and 13a show. After cracking, the flexural strength capacity increased in a pseudolinear way with the increase in fiber percentage, as shown in Figures 12b and 13b. This behavior can be attributed to increased fiber bridging capacity.

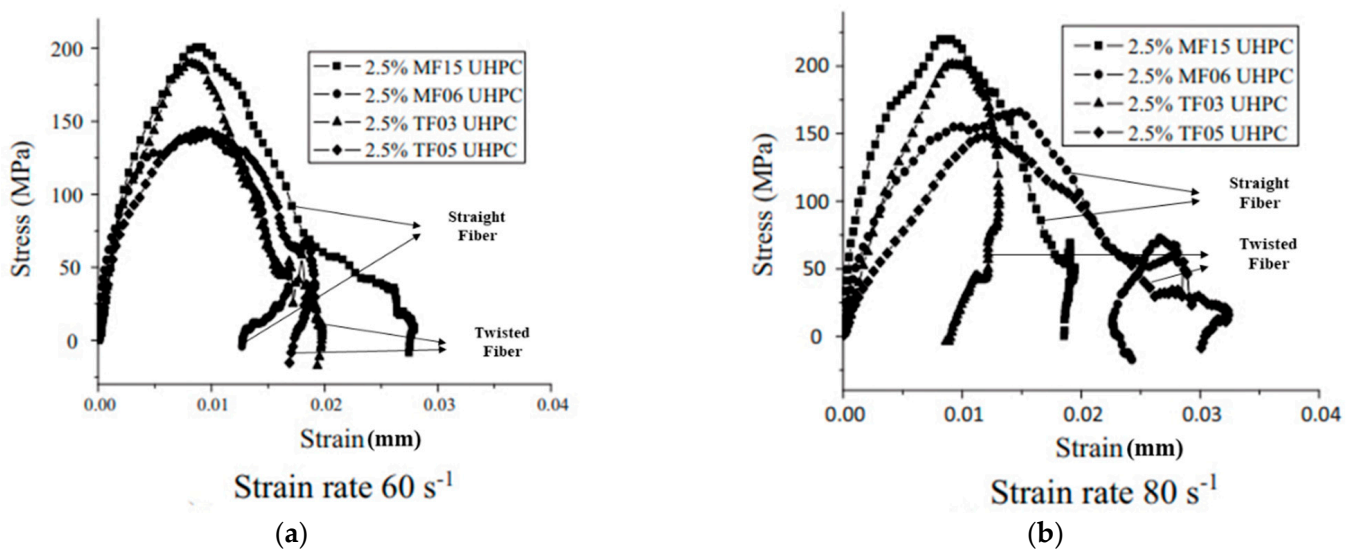


Figure 10. Effects of steel fiber aspect ratios (MF06 = 50, MF15 = 125, TF03 = 100, TF05 = 60) under strain rates of (a)  $60 \text{ s}^{-1}$  and (b)  $80 \text{ s}^{-1}$  [66].

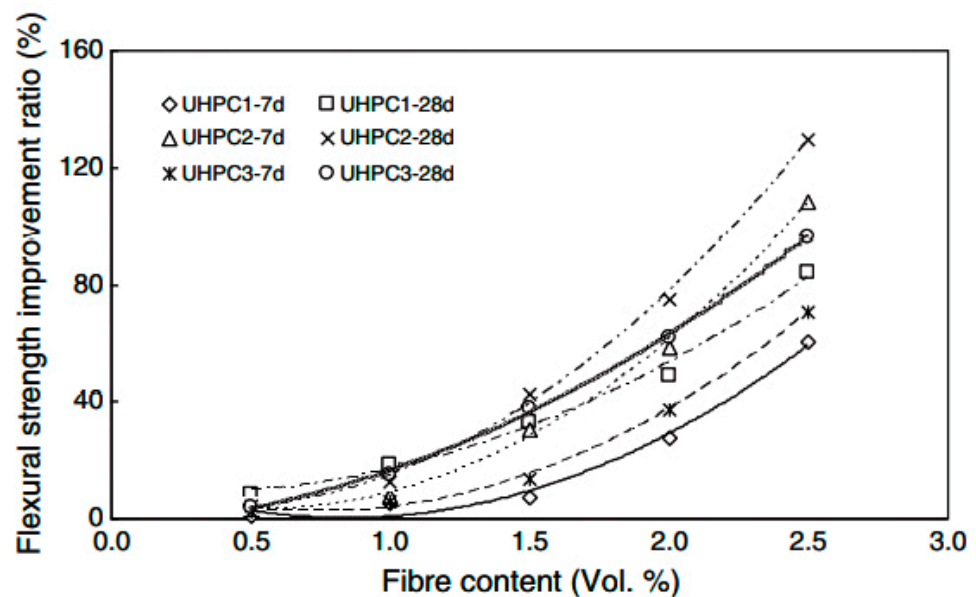


Figure 11. Relation between fiber dosage and flexural strength [48].

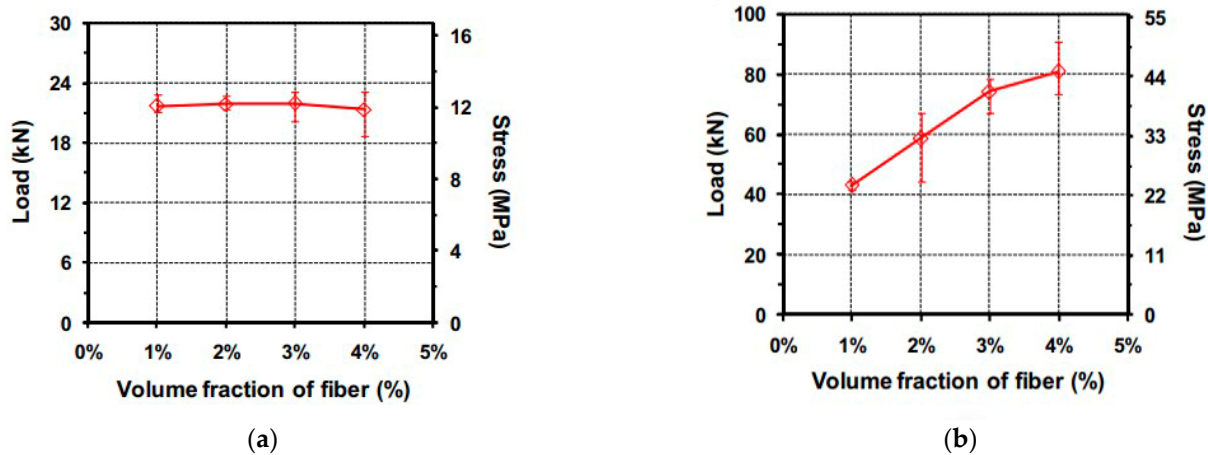


Figure 12. Flexural characteristics of UHPFRC with different fiber dosages: (a) first cracking load, (b) flexural strength [45].

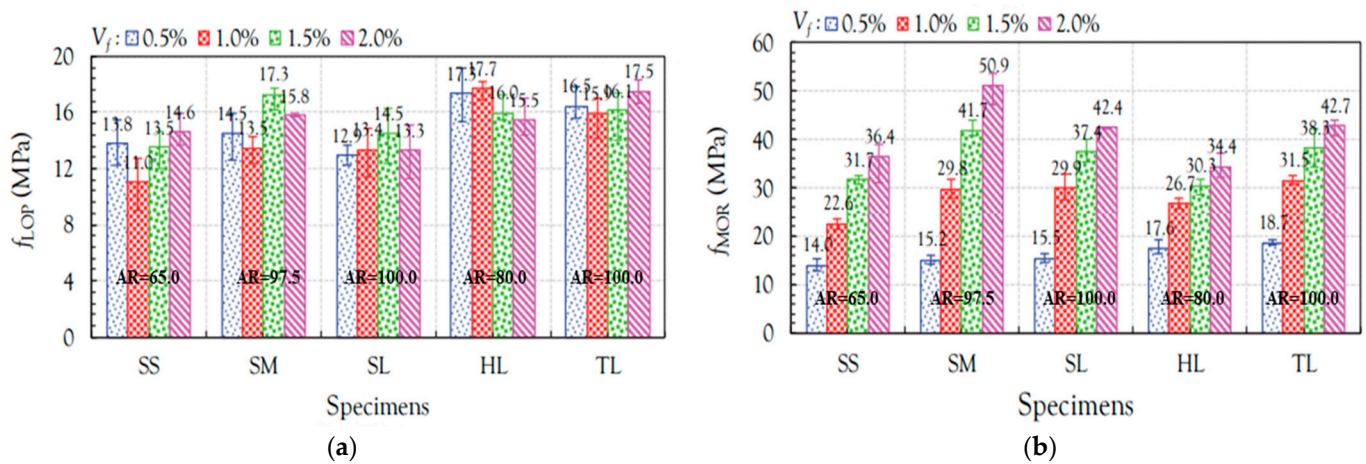


Figure 13. Flexural characteristics of UHPFRC: (a) first cracking condition, (b) post-cracking condition [69].

In addition to examining the influence of steel fiber dosage on the flexural strength of UHPFRC, researchers have also investigated the effects of the aspect ratios of steel fibers on the flexural strength of UHPFRC. Steel fibers with a high aspect ratio demonstrated much improved flexural strength in contrast to that of smaller-aspect ratio steel fibers [38,53,68]. This behavior can be attributed to the larger bonding area in the concrete matrix for longer steel fibers, which leads to increased fiber pullout or slip capacity [39,73]. For instance, Wu et al. [52] measured flexural strength according to GB/T 17671-1999 [74], considering 2% steel fibers with different aspect ratios of 6/0.20 and 13/0.2. Steel fibers with a higher aspect ratio had much better flexural strength than that of steel fibers with a low aspect ratio. In addition, several research groups found that the fiber aspect ratio had negligible impact before the first cracking, as shown in Figure 13a. However, it had a remarkable effect in the post-cracking condition, as illustrated in Figure 13b [35,45,69,75,76]. However, over a certain aspect ratio, the impact of a higher aspect ratio was negative in the post-cracking load condition, as shown in Figure 13b, where specimens SS, SM, SL, HL, and TL had aspect ratios of 65, 97.5, 100, 80, and 100, respectively.

A group of researchers examined the impact of fiber percentage through the weight-drop test and found that the maximal load-bearing capacity increased with an increase in fiber percentage [77,78]. Farnam et al. [78] examined the effects of different fiber percentages through impact load and noted that two samples containing 2% steel fiber content broke after 15 strikes, whereas specimens with 4% steel fibers broke after 30 strikes. On the other hand, Ngo et al. [79] examined the impact of different steel fiber percentages with varying strain rates (6.94 and 13.83 m/s loading rate) and observed that an increase in fiber percentage resulted in increased average peak load (Table 2).

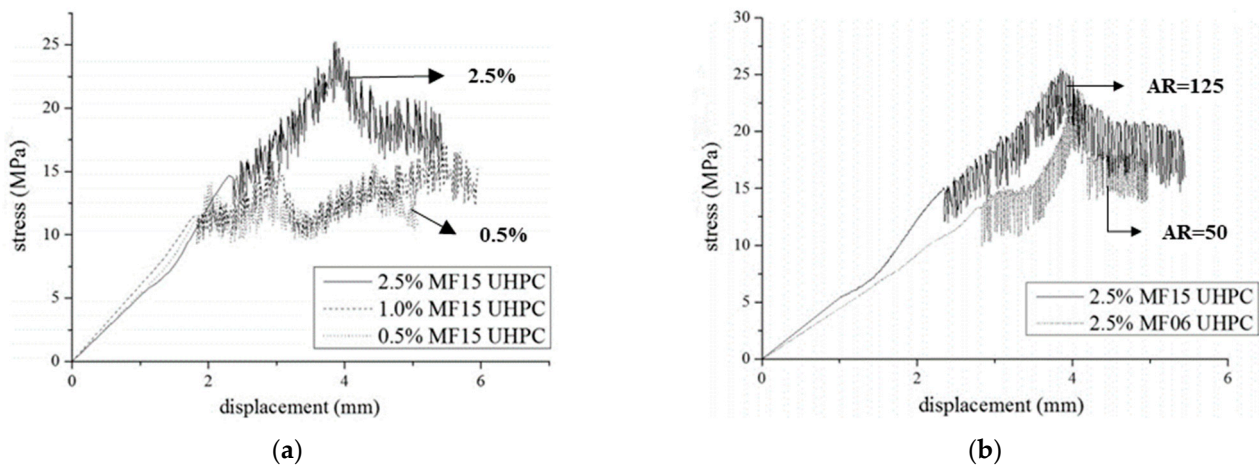
**Table 2.** Effects of fiber percentages and aspect ratios on different loading speed levels [79].

| Sample Series Name | Aspect Ratio | Fiber Percentage | Loading Speed (m/s) | Average Peak Load (KN) |
|--------------------|--------------|------------------|---------------------|------------------------|
| SS                 | 13/0.2       | 0                | 6.94                | 2.75                   |
| SS                 | 13/0.2       | 0.5              | 6.94                | 9.90                   |
| SS                 | 13/0.2       | 1.5              | 6.94                | 11.49                  |
| SS                 | 13/0.2       | 0                | 13.83               | 5.58                   |
| SS                 | 13/0.2       | 0.5              | 13.83               | 14.36                  |
| SS                 | 13/0.2       | 1.5              | 13.83               | 18.88                  |
| LS                 | 19/0.2       | 1.5              | 6.94                | 14.16                  |
| LS                 | 19/0.2       | 1.5              | 13.83               | 22.37                  |

Several researchers also investigated the effect of steel fiber aspect ratio and reported that a larger steel fiber aspect ratio resulted in increased flexural capacity and number of strikes [53,79]. For example, Yu et al. [53] examined dynamic flexural strength using the Charpy impact test and saw that steel fibers with an aspect ratio of 13/0.2 absorbed more impact energy than steel fibers with a 6/0.16 aspect ratio, although steel fibers were constant. Ngo et al. [79] tested flexural strength using different strain rates (6.94 and 13.83 m/s) and noted that higher-aspect-ratio steel fibers (19/0.2) resulted in improved load resistance capacity in contrast to steel fibers with a smaller aspect ratio (13/0.2), as shown in Table 2.

### 3.3. Effects of Steel Fiber Percentages and Aspect Ratios on Split Tensile Strength

Several groups of researchers have observed that an increased dosage of steel fiber has a positive effect on the split tensile strength of UHPFRC [47,58,59,66,80–82]. Su et al. [66] reported that the split tensile strength of a specimen significantly increased when the steel fiber amount increased from 1% to 2.5%, as illustrated in Figure 14a. An experimental program carried out by Shehab El-Din et al. [81] showed that the split tensile strength increased by 66% when the fiber dosage was increased from 0 to 3%.

**Figure 14.** Tensile strength of UHPFRC: (a) different steel fiber percentages; (b) different aspect ratios [66].

Several researchers have examined the impact of the aspect ratio of steel fibers on split tensile strength [66,81,82]. The experimental study carried out by Su et al. [66] revealed that specimen MF 15 (aspect ratio 125) demonstrated higher split tensile strength than that of specimen MF06 (aspect ratio 50), as shown in Figure 14b. Su et al. [66] also observed that larger-aspect ratio steel fibers (MF15 and TF03) had a narrow crack and better resistance capabilities than those of smaller-aspect ratio steel fibers (MF06 and TF05), as shown in Figure 15. Shehab El-Din et al. [81] noted that steel fibers with a high aspect ratio had a significant effect when the specimens were casted with a smaller steel fiber amount (1%), as shown in Table 3. However, it followed a downward trend with an increased steel fiber amount, as shown in Table 3.

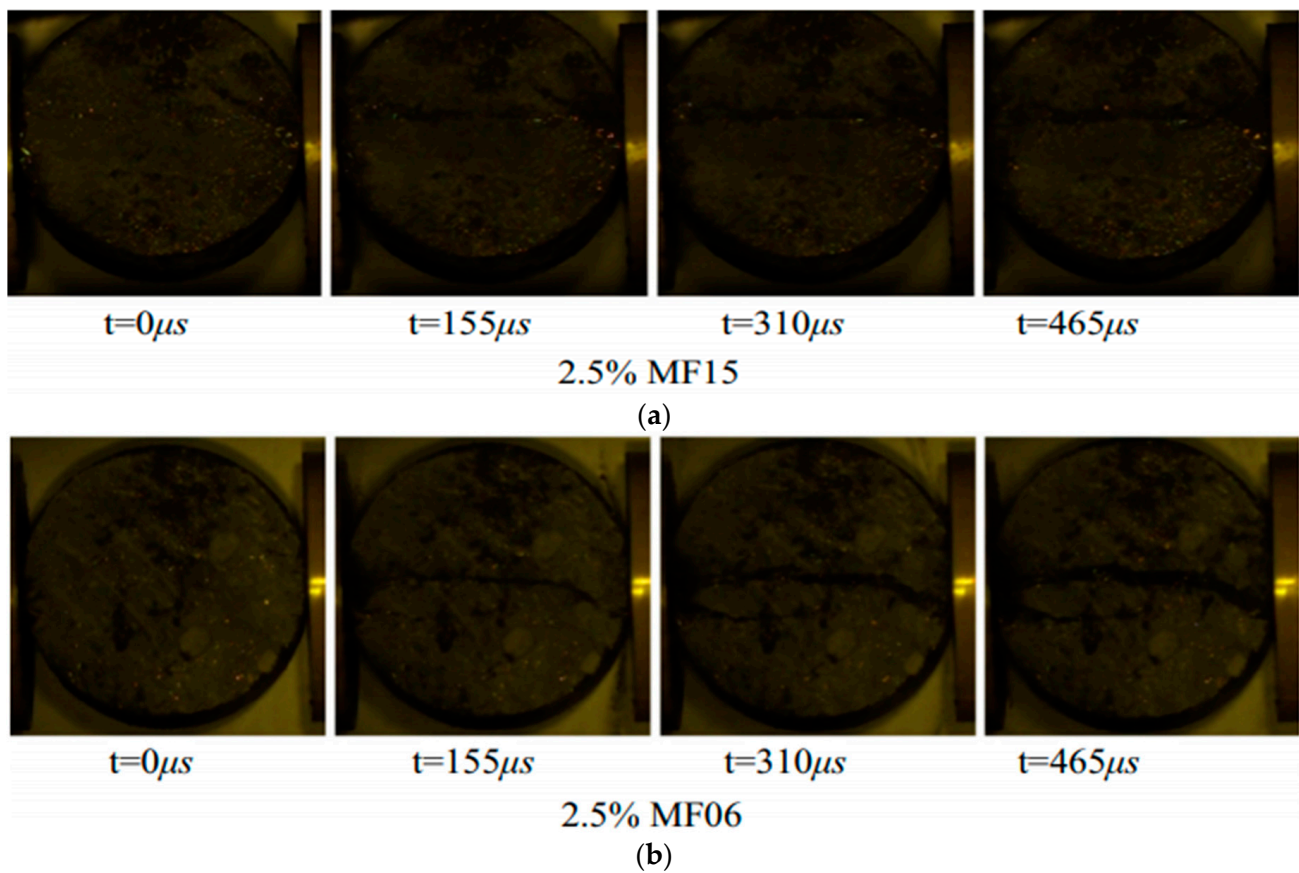


**Figure 15.** Effects of different aspect ratios of steel fibers on crack propagation: (a) MF15 (aspect ratio 125), (b) MF06 (aspect ratio 50) [66].

**Table 3.** Effects of fiber percentages and aspect ratios on split tensile strength [81].

| Sample No | Aspect Ratio | Fiber Percentage | Split Tensile Strength (MPa) | Increased Strength Percentage (Compared to No Fiber Percentage) | Difference Between Two Aspect Ratios Strength Percentage |
|-----------|--------------|------------------|------------------------------|---|--|
| 1         | 0            | 0                | 11.5                         | -   | -  |
| 2         | 30           | 1                | 12.73                        | 10.70   | 23.22  |
| 3         | 50           | 1                | 15.4                         | 33.91   |  |
| 4         | 30           | 2                | 15.59                        | 35.57   | 16.17  |
| 5         | 50           | 2                | 17.45                        | 51.74   |  |
| 6         | 30           | 3                | 17.82                        | 54.96   |  |
| 7         | 50           | 3                | 19.10                        | 66.09   | 11.13  |

#### 4. Conclusions and Future Research Needs

This work conducted an extensive literature review on the distinctive characteristics of ultrahigh-performance fiber-reinforced concrete (UHPFRC). According to the state-of-the-art review and discussions, the following summary can be drawn:

1. Steel fiber amount and aspect ratio significantly influence the workability of UHPFRC. Higher steel fiber percentages and aspect ratios cause interlocking among fibers and ultimately lead to reduced slump flow;
2. The compressive strength of UHPFRC is gradually increased with increased steel fiber dosage for the capability of delaying crack formation and propagation. Nevertheless, improper fiber distribution in a concrete mixture may lead to the decreased compressive strength of UHPFRC;

3. Steel fibers with a high aspect ratio resist crack opening and improve compressive strength. In contrast, steel fibers with a low aspect ratio can only control microcrack opening and propagation;
4. The effects of aspect ratios were examined for flexural and split tensile strength. Higher-aspect ratio steel fibers could improve flexural and split tensile strength with a constant fiber percentage, owing to the large bonding surface between fibers and the concrete matrix;
5. A faster strain rate significantly improved the mechanical properties of UHPFRC.

In addition to the aforementioned conclusions, the following aspects need to be addressed in future research:

1. Extensive research should be carried out to understand the effect of fiber percentage or aspect ratio on the setting time of UHPFRC;
2. Owing to the low water-to-cement ratio, the outer surface of UHPFRC has a much faster evaporation rate than that of the inner surface. Therefore, an accurate measurement method for setting time needs to be developed;
3. Steel fibers significantly influenced the mechanical properties of UHPFRC. Hence, to reduce manufacturing costs, the effects of other factors such as avoiding high-pressure compaction and heat treatments should be further investigated;
4. Because the distribution of steel fibers can affect compressive strength, a proper mixing procedure needs to be developed.

**Author Contributions:** Conceptualization, R.K.B. and F.B.A.; methodology, F.B.A. and R.K.B.; software, F.H. and Z.H.; validation, R.K.B.; formal analysis, A.A.P.; investigation, M.E.H. and Z.H.; resources, M.E.H., A.A.P., Z.H. and F.H.; data curation, M.E.H. and A.A.P.; writing—original draft preparation, F.B.A.; writing—review and editing, R.K.B. and D.S.; visualization, F.B.A. and R.K.B.; supervision, R.K.B. All authors have read and agreed to the published version of the manuscript.

**Funding:** This research received no external funding.

**Institutional Review Board Statement:** Not applicable.

**Informed Consent Statement:** Not applicable.

**Conflicts of Interest:** The authors declare no conflict of interest.

## References

1. Xiao, J.; Qiang, C.; Nanni, A.; Zhang, K. Use of sea-sand and seawater in concrete construction: Current status and future opportunities. *Constr. Build. Mater.* **2017**, *155*, 1101–1111. [[CrossRef](#)]
2. Li, Z. *Advanced Concrete Technology*, 1st ed.; John Wiley & Sons: Hoboken, NJ, USA, 2011.
3. Ragavendra, S.; Reddy, I.P.; Dongre, A.R. Fibre reinforced concrete—A case study. In Proceedings of the Architectural Engineering Aspect for Sustainable Building Envelopes, Khairatabad, Hyderabad, India, 10–11 November 2017; pp. 1–15.
4. Biswas, R.K.; Iwanami, M.; Chijiwa, N.; Uno, K. Effect of non-uniform rebar corrosion on structural performance of RC structures: A numerical and experimental investigation. *Constr. Build. Mater.* **2020**, *230*, 116908. [[CrossRef](#)]
5. Biswas, R.K.; Iwanami, M.; Chijiwa, N.; Uno, K. Finite element analysis of rc beams subjected to non-uniform corrosion of steel bars. In Proceedings of the Fifth International Conference on Sustainable Construction Materials and Technologies, London, UK, 14–17 July 2019.
6. Biswas, R.K.; Iwanami, M.; Chijiwa, N.; Nakayama, K. Numerical evaluation on the effect of steel bar corrosion on the cyclic behaviour of RC bridge piers. *Mater. Today Proc.* **2021**. [[CrossRef](#)]
7. Paul, S.C.; Pirskawetz, S.; Van Zijl, G.P.A.G.; Schmidt, W. Acoustic emission for characterising the crack propagation in strain-hardening cement-based composites (SHCC). *Cem. Concr. Res.* **2015**, *69*, 19–24. [[CrossRef](#)]
8. Paul, S.C.; Babafemi, A.J. A review of the mechanical and durability properties of strain hardening cement-based composite (SHCC). *J. Sustain. Cem. Mater.* **2018**, *7*, 57–78. [[CrossRef](#)]
9. Chao, S.-H.; Liao, W.-C.; Wongtanakitcharoen, T.; Naaman, A.E. Large scale tensile tests of high performance fiber reinforced cement composites. In Proceedings of the Fifth International RILEM Workshop on High Performance Fiber Reinforced Cement Composites (HPFRCC5), Mainz, Germany, 10–13 July 2007; pp. 77–86.
10. Bonopera, M.; Chang, K.-C.; Chen, C.-C.; Sung, Y.-C.; Tullini, N. Prestress force effect on fundamental frequency and deflection shape of PCI beams. *Struct. Eng. Mech. An Int. J.* **2018**, *67*, 255–265.
11. Singh, B.P.; Yazdani, N.; Ramirez, G. Effect of a time dependent concrete modulus of elasticity on prestress losses in bridge girders. *Int. J. Concr. Struct. Mater.* **2013**, *7*, 183–191. [[CrossRef](#)]

12. Bin Ahmed, F.; Biswas, R.K.; Abid Ahsan, K.; Islam, S.; Rahman, M.R. Estimation of strength properties of geopolymers concrete. *Mater. Today Proc.* **2021**, *44*, 871–877. [[CrossRef](#)]
13. Yudenfreund, M.; Odler, I.; Brunauer, S. Hardened portland cement pastes of low porosity I. Materials and experimental methods. *Cem. Concr. Res.* **1972**, *2*, 313–330. [[CrossRef](#)]
14. Roy, D.M.; Gouda, G.R.; Bobrowsky, A. Very high strength cement pastes prepared by hot pressing and other high pressure techniques. *Cem. Concr. Res.* **1972**, *2*, 349–366. [[CrossRef](#)]
15. Alford, N.M.; Birchall, J.D. The properties and potential applications of macro-defect-free cement. *MRS Online Proc. Libr. OPL* **1984**, *42*, 265–276. [[CrossRef](#)]
16. Bache, H.H. *Introduction to Compact Reinforced Composite*; Nordic Concrete Federation: Denmark, 1987.
17. de Larrard, F.; Sedran, T. Optimization of ultra-high-performance concrete by the use of a packing model. *Cem. Concr. Res.* **1994**, *24*, 997–1009. [[CrossRef](#)]
18. Richard, P.; Cheyrezy, M. Composition of reactive powder concretes. *Cem. Concr. Res.* **1995**, *25*, 1501–1511. [[CrossRef](#)]
19. Wille, K.; Naaman, A.E.; Parra-Montesinos, G.J. Ultra-high performance Concrete with compressive strength exceeding 150 MPa (22 ksi): A simpler way. *ACI Mater. J.* **2011**, *108*, 46–54. [[CrossRef](#)]
20. Wille, K.; Naaman, A.E.; El-Tawil, S.; Parra-Montesinos, G.J. Ultra-high performance concrete and fiber reinforced concrete: Achieving strength and ductility without heat curing. *Mater. Struct. Constr.* **2012**, *45*, 309–324. [[CrossRef](#)]
21. Wille, K.; Naaman, A.E.; El-Tawil, S. Optimizing Ultra-High-Performance Fiber-Reinforced Concrete Mixtures with twisted fibers exhibit record performance under tensile loading. *Concr. Int.* **2011**, *33*, 35–41.
22. Russel, H.G.; Graybeal, B.A. *Ultra-High Performance Concrete: A State-of-the-Art Report for the Bridge Community*; Federal Highway Administration, Office of Infrastructure Research and Development: Washington, DC, USA, 2013; pp. 2101–2296.
23. Aghdasi, P.; Heid, A.E.; Chao, S.H. Developing ultra-high-performance fiber-reinforced concrete for large-scale structural applications. *ACI Mater. J.* **2016**, *113*, 559–569. [[CrossRef](#)]
24. Tong, T.; Wang, J.; Lei, H.; Liu, Z. UHPC jacket retrofitting of reinforced concrete bridge piers with low flexural reinforcement ratios: Experimental investigation and three-dimensional finite element modeling. *Struct. Infrastruct. Eng.* **2020**. [[CrossRef](#)]
25. Hanifehzadeh, M.; Aryan, H.; Gencturk, B.; Akyniyazov, D. Structural response of steel jacket-uhpc retrofitted reinforced concrete columns under blast loading. *Materials* **2021**, *14*, 1521. [[CrossRef](#)]
26. Lee, J.Y.; Aoude, H.; Yoon, Y.S.; Mitchell, D. Impact and blast behavior of seismically-detailed RC and UHPFRC-Strengthened columns. *Int. J. Impact Eng.* **2020**, *143*, 103628. [[CrossRef](#)]
27. Charron, J.P.; Denarié, E.; Brühwiler, E. Permeability of ultra high performance fiber reinforced concretes (UHPFRC) under high stresses. *Mater. Struct. Constr.* **2007**, *40*, 269–277. [[CrossRef](#)]
28. Tam, C.M.; Tam, V.W.Y.; Ng, K.M. Assessing drying shrinkage and water permeability of reactive powder concrete produced in Hong Kong. *Constr. Build. Mater.* **2012**, *26*, 79–89. [[CrossRef](#)]
29. Azmee, N.M.; Shafiq, N. Ultra-high performance concrete: From fundamental to applications. *Case Stud. Constr. Mater.* **2018**, *9*, e00197. [[CrossRef](#)]
30. Gosavi, J.S.; Awari, U.R. A Review on High-Performance Concrete. *Int. Res. J. Eng. Technol.* **2018**, *5*, 1965–1968.
31. He, Z.-h.; Du, S.-g.; Chen, D. Microstructure of ultra high performance concrete containing lithium slag. *J. Hazard. Mater.* **2018**, *353*, 35–43. [[CrossRef](#)]
32. Kim, J.K.; Han, S.H.; Song, Y.C. Effect of temperature and aging on the mechanical properties of concrete: Part, I. Experimental results. *Cem. Concr. Res.* **2002**, *32*, 1087–1094. [[CrossRef](#)]
33. Soliman, N.A.; Tagnit-Hamou, A. Development of ultra-high-performance concrete using glass powder—Towards ecofriendly concrete. *Constr. Build. Mater.* **2016**, *125*, 600–612. [[CrossRef](#)]
34. Pyo, S.; Kim, H.K. Fresh and hardened properties of ultra-high performance concrete incorporating coal bottom ash and slag powder. *Constr. Build. Mater.* **2017**, *131*, 459–466. [[CrossRef](#)]
35. Yoo, D.Y.; Kang, S.T.; Yoon, Y.S. Effect of fiber length and placement method on flexural behavior, tension-softening curve, and fiber distribution characteristics of UHPFRC. *Constr. Build. Mater.* **2014**, *64*, 67–81. [[CrossRef](#)]
36. Wille, K.; Kim, D.J.; Naaman, A.E. Strain-hardening UHP-FRC with low fiber contents. *Mater. Struct. Constr.* **2011**, *44*, 583–598. [[CrossRef](#)]
37. Yoo, D.Y.; Banthia, N. Mechanical properties of ultra-high-performance fiber-reinforced concrete: A review. *Cem. Concr. Compos.* **2016**, *73*, 267–280. [[CrossRef](#)]
38. Yoo, D.Y.; Kang, S.T.; Yoon, Y.S. Enhancing the flexural performance of ultra-high-performance concrete using long steel fibers. *Compos. Struct.* **2016**, *147*, 220–230. [[CrossRef](#)]
39. Yoo, D.Y.; Zi, G.; Kang, S.T.; Yoon, Y.S. Biaxial flexural behavior of ultra-high-performance fiber-reinforced concrete with different fiber lengths and placement methods. *Cem. Concr. Compos.* **2015**, *63*, 51–66. [[CrossRef](#)]
40. Ryu, G.S.; Kang, S.T.; Park, J.J.; Koh, K.T.; Kim, S.W. Mechanical behavior of UHPC (ultra high performance concrete) according to hybrid use of steel fibers. *Adv. Mater. Res.* **2011**, *287–290*, 453–457. [[CrossRef](#)]
41. ASTM International. *Standard Test Method for Time of Setting of Concrete Mixtures by Penetration Resistance*; ASTM International: West Conshohocken, PA, USA, 2016.
42. Yoo, D.Y.; Park, J.J.; Kim, S.W.; Yoon, Y.S. Early age setting, shrinkage and tensile characteristics of ultra high performance fiber reinforced concrete. *Constr. Build. Mater.* **2013**, *41*, 427–438. [[CrossRef](#)]

43. Zhang, Y.; Zhang, W.; She, W.; Ma, L.; Zhu, W. Ultrasound monitoring of setting and hardening process of ultra-high performance cementitious materials. *NDT E Int.* **2012**, *47*, 177–184. [[CrossRef](#)]
44. Svec, O.; Pade, C. Ultra high performance fibre reinforced concrete as a waterproofing solution for concrete bridge deck renovations. In Proceedings of the XXII Nordic Concrete Research Symposia, Reykjavik, Iceland, 13–15 August 2014; pp. 273–276.
45. Yoo, D.Y.; Lee, J.H.; Yoon, Y.S. Effect of fiber content on mechanical and fracture properties of ultra high performance fiber reinforced cementitious composites. *Compos. Struct.* **2013**, *106*, 742–753. [[CrossRef](#)]
46. Martinie, L.; Rossi, P.; Roussel, N. Rheology of fiber reinforced cementitious materials: Classification and prediction. *Cem. Concr. Res.* **2010**, *40*, 226–234. [[CrossRef](#)]
47. Abbas, S.; Soliman, A.M.; Nehdi, M.L. Exploring mechanical and durability properties of ultra-high performance concrete incorporating various steel fiber lengths and dosages. *Constr. Build. Mater.* **2015**, *75*, 429–441. [[CrossRef](#)]
48. Yu, R.; Spiesz, P.; Brouwers, H.J.H. Mix design and properties assessment of Ultra-High Performance Fibre Reinforced Concrete (UHPRFC). *Cem. Concr. Res.* **2014**, *56*, 29–39. [[CrossRef](#)]
49. Le Hoang, A.; Fehling, E. Influence of steel fiber content and aspect ratio on the uniaxial tensile and compressive behavior of ultra high performance concrete. *Constr. Build. Mater.* **2017**, *153*, 790–806. [[CrossRef](#)]
50. Arel, H.Ş. Effects of curing type, silica fume fineness, and fiber length on the mechanical properties and impact resistance of UHPRFC. *Results Phys.* **2016**, *6*, 664–674. [[CrossRef](#)]
51. Rossi, P. Development of new cement composite materials for construction. *Proc. Inst. Mech. Eng. Part L J. Mater. Des. Appl.* **2005**, *219*, 67–74. [[CrossRef](#)]
52. Wu, Z.; Shi, C.; He, W.; Wang, D. Static and dynamic compressive properties of ultra-high performance concrete (UHPC) with hybrid steel fiber reinforcements. *Cem. Concr. Compos.* **2017**, *79*, 148–157. [[CrossRef](#)]
53. Yu, R.; Spiesz, P.; Brouwers, H.J.H. Static properties and impact resistance of a green Ultra-High Performance Hybrid Fibre Reinforced Concrete (UHPRFC): Experiments and modeling. *Constr. Build. Mater.* **2014**, *68*, 158–171. [[CrossRef](#)]
54. Schmidt, M.; Fehling, E.; Teichmann, T.; Bunje, K.; Bornemann, R. Ultra-high performance concrete: Perspective for the precast concrete industry | Request PDF. *Concr. Precast. Plant Tech* **2003**, *69*, 16–29.
55. Abbas, S.; Nehdi, M.L.; Saleem, M.A. Ultra-high performance concrete: Mechanical performance, durability, sustainability and implementation challenges. *Int. J. Concr. Struct. Mater.* **2016**, *10*, 271–295. [[CrossRef](#)]
56. Yoo, D.Y.; Shin, H.O.; Yang, J.M.; Yoon, Y.S. Material and bond properties of ultra high performance fiber reinforced concrete with micro steel fibers. *Compos. Part B Eng.* **2014**, *58*, 122–133. [[CrossRef](#)]
57. Rong, Z.; Sun, W.; Zhang, Y. Dynamic compression behavior of ultra-high performance cement based composites. *Int. J. Impact Eng.* **2010**, *37*, 515–520. [[CrossRef](#)]
58. Gesoglu, M.; Güneş, E.; Muhyaddin, G.F.; Asaad, D.S. Strain hardening ultra-high performance fiber reinforced cementitious composites: Effect of fiber type and concentration. *Compos. Part B Eng.* **2016**, *103*, 74–83. [[CrossRef](#)]
59. Jin, L.; Zhang, R.; Tian, Y.; Dou, G.; Du, X. Experimental investigation on static and dynamic mechanical properties of steel fiber reinforced ultra-high-strength concretes. *Constr. Build. Mater.* **2018**, *178*, 102–111. [[CrossRef](#)]
60. Ibrahim, M.A.; Farhat, M.; Issa, M.A.; Hasse, J.A. Effect of material constituents on mechanical & fracture mechanics properties of ultra-high-performance concrete. *ACI Struct. J.* **2017**, *114*, 453–465. [[CrossRef](#)]
61. Wang, R.; Gao, X. Relationship between flowability, entrapped air content and strength of UHPC mixtures containing different dosage of steel fiber. *Appl. Sci.* **2016**, *6*, 216. [[CrossRef](#)]
62. Kazemi, S.; Lubell, A.S. Influence of Specimen Size and Fiber Content on Mechanical Properties of Ultra-High-Performance Fiber-Reinforced Concrete. *ACI Mater. J.* **2012**, *109*. [[CrossRef](#)]
63. ASTM International. *Standard Test Method for Compressive Strength of Hydraulic Cement Mortars (Using 2-in. or [50 mm] Cube Specimens)*; ASTM International: West Conshohocken, PA, USA, 2020.
64. ASTM International. *Standard Test Method for Compressive Strength of Cylindrical Concrete Specimens*; ASTM International: West Conshohocken, PA, USA, 2021.
65. Liao, W.C.; Perceka, W.; Liu, E.J. Compressive stress-strain relationship of high strength steel fiber reinforced concrete. *J. Adv. Concr. Technol.* **2015**, *13*, 379–392. [[CrossRef](#)]
66. Su, Y.; Li, J.; Wu, C.; Wu, P.; Li, Z.X. Effects of steel fibres on dynamic strength of UHPC. *Constr. Build. Mater.* **2016**, *114*, 708–718. [[CrossRef](#)]
67. Lai, J.; Sun, W. Dynamic behaviour and visco-elastic damage model of ultra-high performance cementitious composite. *Cem. Concr. Res.* **2009**, *39*, 1044–1051. [[CrossRef](#)]
68. Park, J.J.; Yoo, D.Y.; Park, G.J.; Kim, S.W. Feasibility of reducing the fiber content in ultra-high-performance fiber-reinforced concrete under flexure. *Materials* **2017**, *10*, 118. [[CrossRef](#)]
69. Yoo, D.Y.; Kim, S.; Park, G.J.; Park, J.J.; Kim, S.W. Effects of fiber shape, aspect ratio, and volume fraction on flexural behavior of ultra-high-performance fiber-reinforced cement composites. *Compos. Struct.* **2017**, *174*, 375–388. [[CrossRef](#)]
70. ASTM International. *Standard Test Method for Flexural Performance of Fiber-Reinforced Concrete (Using Beam with Third-Point Loading)*; ASTM International: West Conshohocken, PA, USA, 2019.
71. ASTM International. *Standard Test Method for Flexural Toughness and First-Crack Strength of Fiber-Reinforced Concrete (Using Beam with Third-Point Loading)*; ASTM International: West Conshohocken, PA, USA, 1997.

72. Wu, Z.; Shi, C.; He, W.; Wu, L. Effects of steel fiber content and shape on mechanical properties of ultra high performance concrete. *Constr. Build. Mater.* **2016**, *103*, 8–14. [[CrossRef](#)]
73. Yoo, D.-Y.; Banthia, N.; Zi, G.; Yoon, Y.-S. Comparative biaxial flexural behavior of ultra-high-performance fiber-reinforced concrete panels using two different test and placement methods. *J. Test. Eval.* **2017**, *45*, 624–641. [[CrossRef](#)]
74. *Method of Testing Cement-Determination of Strength*. GB National Standard; GB/T 17671-1999; AQSIQ: China, 1999.
75. Yunsheng, Z.; Wei, S.; Sifeng, L.; Chujie, J.; Jianzhong, L. Preparation of C200 green reactive powder concrete and its static-dynamic behaviors. *Cem. Concr. Compos.* **2008**, *30*, 831–838. [[CrossRef](#)]
76. Kang, S.T.; Lee, Y.; Park, Y.D.; Kim, J.K. Tensile fracture properties of an Ultra High Performance Fiber Reinforced Concrete (UHPRFC) with steel fiber. *Compos. Struct.* **2010**, *92*, 61–71. [[CrossRef](#)]
77. Yoo, D.Y.; Yoon, Y.S.; Banthia, N. Flexural response of steel-fiber-reinforced concrete beams: Effects of strength, fiber content, and strain-rate. *Cem. Concr. Compos.* **2015**, *64*, 84–92. [[CrossRef](#)]
78. Farnam, Y.; Shekarchi, M.; Mirdamadi, A. Experimental investigation of impact behaviour of high strength fiber reinforced concrete panels. In Proceedings of the 2nd International Symposium on Ultra-High Performance Concrete, Kassel, Germany, 5–7 March 2008; pp. 751–758.
79. Ngo, T.T.; Park, J.K.; Kim, D.J. Loading rate effect on crack velocity in ultra-high-performance fiber-reinforced concrete. *Constr. Build. Mater.* **2019**, *197*, 548–558. [[CrossRef](#)]
80. Prem, P.R.; Bharatkumar, B.H.; Iyer, N.R. Mechanical Properties of Ultra High Performance Concrete. *Int. J. Civ. Environ. Eng.* **2012**, *6*, 676–685.
81. El-Din, H.S.; Mohamed, H.; Khater, M.A.E.-H.; Ahmed, S. Effect of Steel Fibers on Behavior of Ultra High Performance Concrete. In *International Interactive Symposium on Ultra-High Performance Concrete*; Iowa State University Digital Press: Iowa, IA, USA, 2016; pp. 1–10.
82. Sudarshan, N.M.; Rao, T.C. Experimental investigations on tensile strength behavior and microstructure of ultra-high-performance fiber-reinforced concrete. *SN Appl. Sci.* **2019**, *1*, 1–11. [[CrossRef](#)]